AFRL-AFOSR-VA-TR-2024-0023

Quantifying the Defect Character of Grain Boundaries with Traction-based Descriptors

Chew, Huck Beng
UNIVERSITY OF ILLINOIS
506 S WRIGHT ST
URBANA, IL, 61801
USA

11/01/2023
Final Technical Report

DISTRIBUTION A: Distribution approved for public release.

Air Force Research Laboratory
Air Force Office of Scientific Research
Arlington, Virginia 22203
Air Force Materiel Command

REPORT DOCUMENTATION PAGE

PLEASE DO NOT RETURN YOUR FORM TO THE ABOVE ORGANIZATION.

1. REPORT DATE	**2. REPORT TYPE**	**3. DATES COVERED**	
20231101	Final	**START DATE** 20190701	**END DATE** 20230630

4. TITLE AND SUBTITLE
Quantifying the Defect Character of Grain Boundaries with Traction-based Descriptors

5a. CONTRACT NUMBER	**5b. GRANT NUMBER**	**5c. PROGRAM ELEMENT NUMBER**
FA9550-19-1-0242		61102F
5d. PROJECT NUMBER	**5e. TASK NUMBER**	**5f. WORK UNIT NUMBER**

6. AUTHOR(S)
Huck Beng Chew

7. PERFORMING ORGANIZATION NAME(S) AND ADDRESS(ES)	**8. PERFORMING ORGANIZATION REPORT NUMBER**
UNIVERSITY OF ILLINOIS 506 S WRIGHT ST URBANA, IL 61801 USA	

9. SPONSORING/MONITORING AGENCY NAME(S) AND ADDRESS(ES)	**10. SPONSOR/MONITOR'S ACRONYM(S)**	**11. SPONSOR/MONITOR'S REPORT NUMBER(S)**
Air Force Office of Scientific Research 875 N. Randolph St. Room 3112 Arlington, VA 22203	AFRL/AFOSR RTB1	AFRL-AFOSR-VA-TR-2024-0023

12. DISTRIBUTION/AVAILABILITY STATEMENT
A Distribution Unlimited: PB Public Release

13. SUPPLEMENTARY NOTES

14. ABSTRACT
Interfaces are ubiquitous in a wide range of natural and engineering materials, and affect many of the mechanical properties. It is well accepted that the grain boundary interfaces control the strength and ductility of nanostructured materials. The objectives of this research is to develop traction- or stress-based grain boundary descriptors to bridge the gap between the defect character at the boundary and the underpinning stress-controlled deformation mechanisms. Such descriptors will ultimately pave the way towards: (a) detailed understanding of the unitmechanisms associated with the relevant defect type at the grain boundary, and (b) the development of predictive models at the meso-scale to quantitatively assess the contribution of such defects to the strength and ductility of the nanostructured material. In this 4-year research project, we have (1) constructed novel grain boundary descriptors for twisted heterogeneous atomic-sheet interfaces, which has enabled the controlled nanomanufacturing of these 2D sheets, (2) extended the notion of local atomistic stress as defined by virial theorem beyond the MD domain, to elucidate the local stress states of grain boundaries modeled in DFT calculations or imaged in a TEM, and (3) obtained a dislocation representation of low- to hightilt-angle grain boundaries from the local atomistic stress fields for direct meso-scale modeling of these boundaries in discrete dislocation dynamics simulations.

15. SUBJECT TERMS

16. SECURITY CLASSIFICATION OF:			**17. LIMITATION OF ABSTRACT**	**18. NUMBER OF PAGES**
a. REPORT	**b. ABSTRACT**	**c. THIS PAGE**	UU	8
U	U	U		

19a. NAME OF RESPONSIBLE PERSON	**19b. PHONE NUMBER** *(Include area code)*
ALI SAYIR	426-7236

Standard Form 298 (Rev.5/2020)
Prescribed by ANSI Std. Z39.18

Final Report for AFOSR FA9550-19-1-0242

Quantifying the Defect Character of Grain Boundaries with Traction-based Descriptors

.

PI: Huck Beng Chew
Department of Aerospace Engineering
University of Illinois at Urbana-Champaign

.

Period Covered: 7/1/2019 through 6/30/2023

1. Accomplishments

Interfaces are ubiquitous in a wide range of natural and engineering materials, and affect many of the mechanical properties. It is well accepted that the grain boundary interfaces control the strength and ductility of nanostructured materials. The objectives of this research is to develop traction- or stress-based grain boundary descriptors to bridge the gap between the defect character at the boundary and the underpinning stress-controlled deformation mechanisms. Such descriptors will ultimately pave the way towards: (a) detailed understanding of the unit-mechanisms associated with the relevant defect type at the grain boundary, and (b) the development of predictive models at the meso-scale to quantitatively assess the contribution of such defects to the strength and ductility of the nanostructured material.

In this 4-year research project, we have (1) constructed novel grain boundary descriptors for twisted heterogeneous atomic-sheet interfaces, which has enabled the controlled nanomanufacturing of these 2D sheets, (2) extended the notion of local atomistic stress as defined by virial theorem beyond the MD domain, to elucidate the local stress states of grain boundaries modeled in DFT calculations or imaged in a TEM, and (3) obtained a dislocation representation of low- to high-tilt-angle grain boundaries from the local atomistic stress fields for direct meso-scale modeling of these boundaries in discrete dislocation dynamics simulations.

The support of this research has led to the following publications:

(1) VanSickle, R., Foehring, D., Chew, H.B., Lambros, J., Microstructure effects on fatigue crack growth in additively manufactured Ti-6Al-4V. *Materials Science and Engineering*: A, 795 (2020), 139993.

(2) Bagchi, S., Johnson, H.T., Chew, H.B., Rotational stability of twisted bilayer graphene. *Physical Review B*, 101 (2020), 054109.

(3) Bagchi, S., Johnson, H.T., Chew, H.B., Strain-controlled rotation of twisted 2D atomic layers for tunable nanomechanical systems. *ACS Applied Nano Materials*, 3 (2020), 10878-10884.

(4) Cui, Y., Chew, H.B., Machine-learning prediction of atomistic stress along grain boundaries. *Acta Materialia*, 222 (2022), 117387.

(5) Noh, W., Chew, H.B., Dislocation descriptors of low and high angle grain boundaries with convolutional neural networks. Submitted (2023).

(6) Cui, Y., Quantifying grain boundary structure-property relationships with atomistic simulations and data driven approaches. Ph.D. Thesis (2022), Department of Aerospace Engineering, University of Illinois at Urbana-Champaign.

(7) Bagchi, S., Mechanics of interfaces in graphene-based nanomaterials. Ph.D. Thesis (2020), Department of Aerospace Engineering, University of Illinois at Urbana-Champaign.

The supported graduate students from this project have received the following research awards:

(8) Dr. Yue Cui – AE Outstanding Graduate Student (2020), Aerospace Alumni Advisory Board Fellowship (2021)

(9) Dr. Soumendu Bagchi – Computer Science & Engineering Fellowship (2019), AE Outstanding Graduate Student (2018), Kenneth Lee Herrick Memorial Award (2020)

Research has also been disseminated to the public in the following conferences:

(10) Yue, C., Chew, H.B. Prediction of grain boundary dislocation emission using machine learning approach. Society of Engineering Sciences 2019

(11) Bagchi, S., Chew, H.B., Mechanisms of interfacial load transfer in graphene based nanocomposites. Society of Engineering Sciences 2019
(12) Bagchi, S., Johnson, H., Chew, H.B., Size dependent stability and thermal motion of moire in twisted bilayer graphene. Society of Engineering Sciences 2019
(13) Qu, W., Bagchi, S., Chen, X., Chew, H.B., Ke, C., Bending and interlayer shear moduli of ultrathin boron nitride nanosheets. ASME IMECE 2019.
(14) Vieira, R.B., Noh, W., Chew, H.B., Lambros, J., Machine-learning neural-network predictions for microscale strain accumulation in polycrystalline metals. MRS Spring 2023.
(15) Noh, W., Cui, Y., Chew, H.B., Quantifying the atomistic structure of grain boundaries with machine learning. Society for Engineering Science, 2023.

Research has also been disseminated to the public through the following invited presentations:

(16) NSF Workshop on Application of Machine Learning to Experimental Mechanics and Materials, Arlington, VA., 2019
(17) Department of Mechanics and Industrial Engineering, New Jersey Institute of Technology, 2022
(18) Department of Mechanical Engineering, National University of Singapore, 2022
(19) Engineering Mechanics Seminar, Institute of High Performance Computing, Singapore, 2022
(20) Department of Mechanical Engineering, Georgia Institute of Technology, 2022
(21) Department of Materials Science & Engineering, University of Tennessee, Knoxville, 2023
(22) Society of Engineering Science, Symposium 5.2. Advances in Multiscale Modeling and Machine Learning in Nanomechanics, 2023

2. Technical Advancement

The major technical advancement we have achieved through this project is (a) the ability to quantify the grain boundary stress field from atomistic simulations (MD, DFT) and experiments (HRTEM), and (b) the ability to use this stress field to establish the dislocation structure of the grain boundary. This has significant implications in the: (1) establishment of the atomistic constitutive law for the bridging of scales between DFT and MD simulations to provide a definition of the quantum-mechanical stress, as well as the bridging between electron microscopy experiments and MD simulations for image-based computation of the atomistic stress, (2) broader interpretation of atomistic stress as a measure of the mechanical stress at the nanoscale beyond classical MD simulations, (3) representation of the atomistic structures of grain boundaries, in terms of unit dislocations as fundamental elements of the boundary, pacing the way for the bridging of scales between MD or DFT models of grain boundaries and mesoscale DDD calculations, and (4) accurate quantification of the dislocation structures of grain boundaries, and hence the local strain distributions, providing rich fundamental insights into the underpinning dislocation mechanics to enable grain boundary engineering.

2.1 A novel approach to quantifying the atomistic stress along grain boundaries

The atomistic stress state along a grain boundary can be treated as a representation of the Cauchy stress tensor for the calculation of continuum traction fields, which ultimately governs the ability of grain boundaries to generate, absorb, or transmit dislocations. Such quantitative grain boundary descriptors are mostly confined to molecular dynamics (MD) simulations where the notion of atomistic stress can be defined through virial theorem. As part of this project, we use artificial neural networks for machine learning (ML), fed with a limited training dataset from MD simulations, to predict the local atomistic stresses from atomic position information across a series of equilibrium <110> symmetrical-tilt Cu grain boundary structures. Accuracy of the ML algorithm is found to depend on the type, sequence, geometry, and orientation of the grain boundary structural units. Accounting for these characteristics in the training dataset enables accurate predictions of the local atomistic stress distributions across the family of grain boundary structures. This ML-based constitutive modeling paves the way for direct interpretation of the equivalent stress state of atomistic structures beyond the MD domain, including those from high-resolution transmission electron microscopy (HRTEM) imaging and Density Functional Theory (DFT) modeling.

The definition of Cauchy stress is fundamental to mechanical property measurements. Similarly, the concept of atomistic stress as a representation of mechanical stress is central to the quantification and interpretation of mechanics-based phenomena at the nanoscale. However, measurements of atomistic stresses to-date are largely confined to molecular dynamics (MD) simulations, which are governed by interatomic potentials for direct computations of an "interatomic force" quantity. We attempt to formulate the "constitutive response" relating atomistic configuration to atomistic stress through a machine learning (ML) approach based on artificial neural networks (ANN). Using ANN, we are able to predict the local atomistic stresses directly from local atomic configuration data along a range of symmetrical-tilt grain boundary structures. These grain boundary atomistic stresses are important quantitative descriptors which govern the deformation mechanics of grain boundaries, including the absorption, emission, and transmission of dislocations.

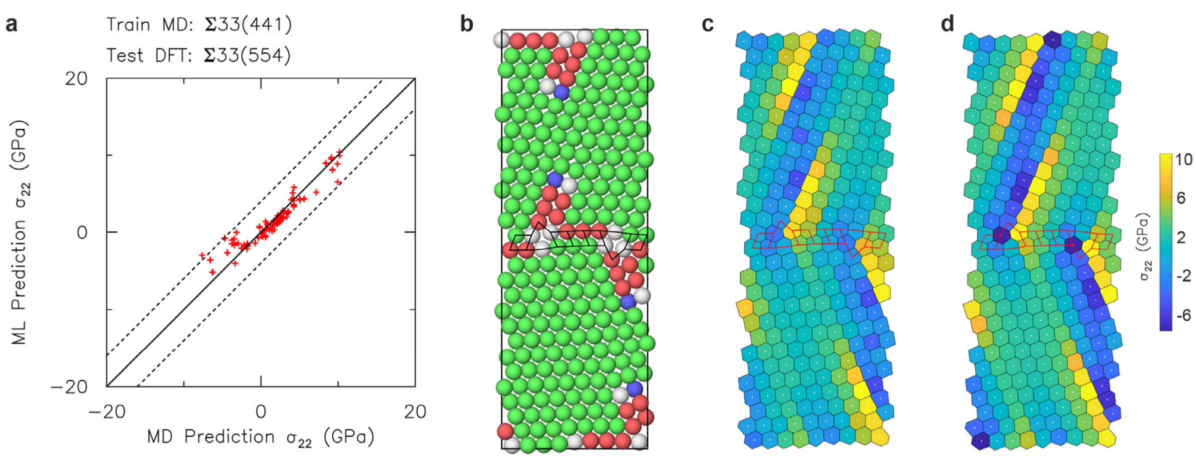

FIG. 1. Atomistic stress σ_{22} predictions of a DFT-computed $\Sigma 33(554)$ grain boundary by ANN trained on MD-computed equilibrium and deformed $\Sigma 33(441)$ grain boundary ($|\epsilon_{22}| = 0, 3\%$). (a) Comparison of the ANN-predicted versus MD-generated σ_{22} atomistic stresses based on structural configuration from DFT. Solid line denotes perfect fitting; dashed lines denote ± 4 GPa error bounds. (b) Final atomic configuration of $\Sigma 33(554)$ grain boundary from DFT and colored according to CNA (Green: FCC, Red: HCP, Blue: BCC, White: other coordination structure). (c) Contours of the ANN-predicted σ_{22} atomistic stresses and (d) MD-generated σ_{22} atomistic stresses of the atomic configuration from DFT.

Generally, ML models require large amounts of data for training. Our results demonstrate that the atomistic stresses in a wide range of grain boundary structures can be accurately predicted by an ANN, trained only on a single grain boundary structure. This is achieved through (1) an

ANN architecture that accounts for invariance in the atomistic stress in the rotated coordinate system with respect to mirror or rotational symmetries in the atomistic configurations, as well as (2) strategic selection or design of training datasets based on the structural unit (SU) type, sequence, and distortion. In particular, we find through our ML predictions that the absence of a SU type or a particular SU sequence between the training and testing datasets can result in significant errors in stress predictions. Designing a training set based on multiple different grain boundary structures generally improves the ANN predictions, but errors still arise from the different extents of SU distortions across the grain boundaries even for training and testing datasets with the same SU type and sequencing. One effective approach we have uncovered is to supplement the equilibrium grain boundary structure used in the training dataset with its deformed configurations under external tension and compression loading. Inclusion of additional deformation data allows for interpolation between the different shapes and sizes of the SUs to significantly improve predictions of the ANN. Surprisingly, even a training set based on an ideal grain boundary structure possessing relatively short grain boundary period length L_p is capable of accurately predicting the atomistic stresses along more complex and longer period random grain boundary structures with zig-zag segments. By extension, the predictions will likely improve for an ANN trained on a more complex random grain boundary structure subjected to additional deformation states (e.g. shear).

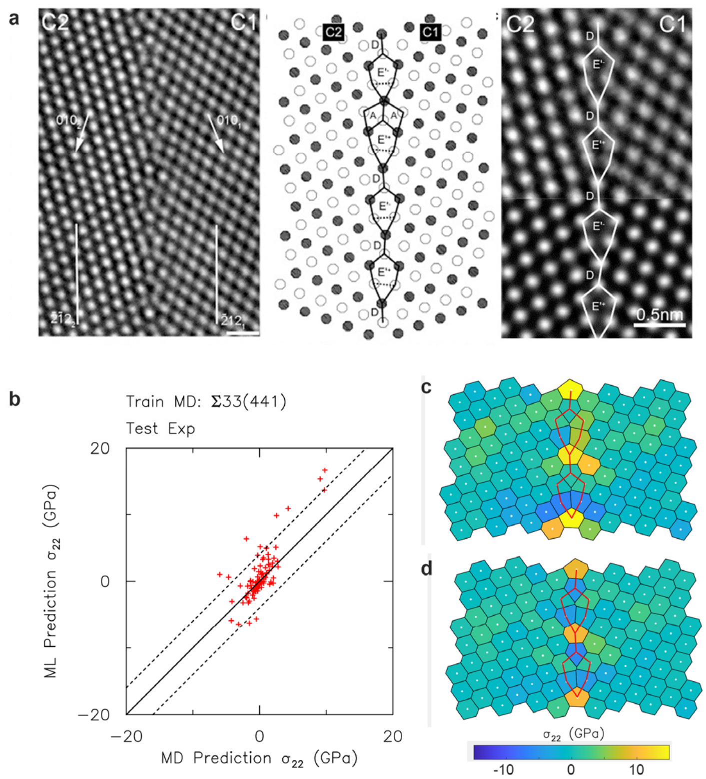

FIG. 2. Atomistic stress σ_{22} predictions from image data by ANN trained on MD-computed equilibrium and deformed $\Sigma33(441)$ grain boundary ($|\epsilon_{22}| = 0, 5\%$). (a) HRTEM image of a symmetrical {221} grain boundary structure (left), with the corresponding simulated energy-minimized structure (middle), and a superposed image of the experimental micrograph and the simulated structure (right) (Duparc et al., 2007). (b) Comparison of the ANN-predicted versus MD-generated σ_{22} atomistic stresses. Solid line denotes perfect fitting; dashed lines denote ± 4 GPa error bounds. (c,d) Contours of the ANN-predicted (c) versus the MD predicted (d) σ_{22} atomistic stresses.

One potentially important application of this ML-based constitutive modeling is in the bridging of scales between different simulation models as well as between simulations and experiments. To illustrate the former, we show in Fig. 1 the direct prediction of the elusive "quantum-mechanical" stress of a $\Sigma33(554)$ grain boundary structure modeled with density functional theory (DFT) calculations, based on an ANN trained on the equilibrium and deformed ($|\epsilon_{22}| = 0, 3\%$) atomistic stress data of a $\Sigma33(441)$ grain boundary from MD simulations. Because of computational limitations, the DFT supercell shown in Fig. 1b is much smaller than the MD simulation box and comprises of 258 Cu atoms with model dimensions of $2.05 \times 5.88 \times 0.26$ nm^3

in the $x_1 \times x_2 \times x_3$ directions. Geometrical relaxations of the supercell are performed using the conjugate gradient method with a force residual of 0.01 eV/Å. Because of the limited simulation supercell size, the shorter ~2.9 nm vertical separation distance between the upper and lower grain boundaries induces the emission of partial dislocations from the E SUs. Despite this irregularity, our ANN-predictions of the quantum-mechanical σ_{22} stresses are in excellent agreement with MD computations of virial stress with an EAM potential based on the actual DFT configuration of the $\Sigma 33(554)$ grain boundary structure. As shown in Fig. 1a, all prediction errors reside well within the ± 4 GPa error bound. The predicted spatial distribution of σ_{22} stresses from our ANN (Fig. 1c) are also quantitatively in very good agreement with the EAM-based virial stress calculations in MD (Fig. 1d). By bridging of scales between DFT and MD simulations, this ML-based approach complements the current array of sophisticated analytical or numerical tools for enabling direct interpretation of the equivalent local quantum-mechanical stress state in DFT.

Recent experimental efforts have focused on elucidating the intrinsic stress and strain information with in situ mechanical tests performed in a TEM. Techniques utilizing moving dislocations as mechanical probes to achieve sub-nanometer strain resolution measurement have been proposed, where their curvature and interactions with other defects could return local stress measurements without interfering with observations. Other techniques include image-based strain and stress measurement through digital image correlation or dark-field in-line holography. We remark that our ML-based predictions of atomistic stress from atomic configurational data obtained experimentally could complement these ongoing experimental efforts. Figure 2a shows a HRTEM image of a symmetrical $\{221\}$ Cu grain boundary structure (left), and a simulated energy-minimized structure of the image (middle), along with a close-up view of the experimental micrograph and a superposed image of the simulated structure at the bottom (right). The observed grain boundary structure is not the lowest energy structure and is a metastable grain boundary. We extract the atomic position data directly from Fig. 2a (middle) which forms the input to our ANN, trained on the atomistic stress data of a $\Sigma 33(441)$ grain boundary with $|\epsilon_{22}| = 0{,}5\%$ from MD simulations. Our ML-based prediction of the atomistic stresses in Fig. 2b generally follows the same trend as MD simulated stresses based on the atomic position data from Fig. 2a. The predicted (ANN) and simulated (MD) spatial distributions of σ_{22} stresses in Fig. 2c and 2d are also very similar. Not surprisingly, the highest error originates from atoms comprising the D-SU, which is not in our training dataset. Nevertheless, these results demonstrate the capability of ML models to achieve direct atomistic stress prediction from atomic position data established experimentally, such as from dark-field electron microscopy.

2.2 Dislocation descriptors of grain boundaries

The notion of grain boundary dislocations (GBDs) as fundamental elements of a grain boundary structure that create the tilt and twist misorientation adjoining the boundary of two crystalline lattices has been well demonstrated by way of atomistic simulations and TEM experiments. These GBDs in turn generate the atomistic field stresses near the grain boundary, which control fundamental mechanistic processes of dislocation emission, absorption, and pile-up, etc. Elucidating the dislocation structure of a boundary from the grain boundary field stresses is therefore an inverse problem, which is particularly challenging for high-tilt-angle grain boundaries due to the overlapping core fields of adjacent GBDs. Our results show that the presence and location of these GBDs across low- to high-tilt-angle grain boundaries can be established with high confidence using convolutional neural networks (CNNs), trained on a dataset generated by superposing the continuum stress fields of unit dislocations. Our predictions capture the transition from sparsely-separated dislocations in low angle grain boundaries, to dislocation clusters with overlapping, polymorphic cores in high angle grain boundaries.

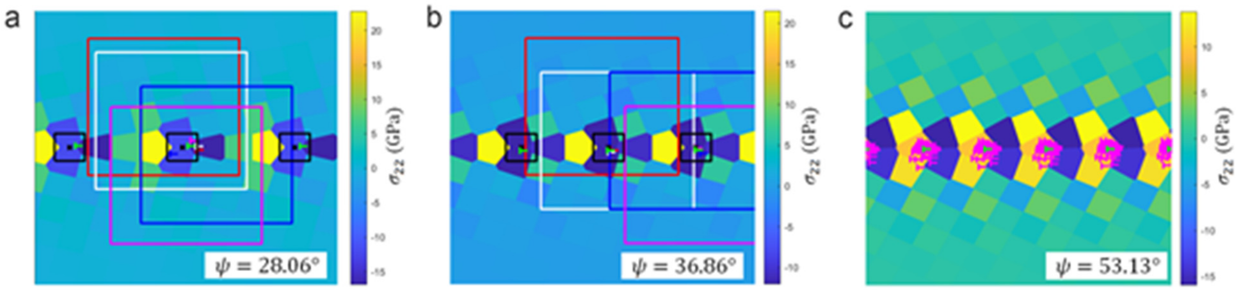

FIG. 3: Dislocation structures of high-tilt-angle grain boundaries from CNN trained on the superposed continuum stress fields of isolated dislocations. Colored boxes and dislocation symbols: sampling of detection windows for true positive edge dislocation with corresponding dislocation locations; black box: ±2 pixel error bound centered about the actual dislocation location (black cross); green dislocation symbol: average predicted dislocation location across all positive detection windows.

Discrete dislocation dynamics (DDD) simulations almost universally ignore core effects, and base the stress field around a dislocation on the analytical linear elastic Volterra solution. However, studies have shown that core effects can be significant ~10 to 50b (~30 to 150 Å) from the dislocation line. This has motivated the development of analytical solutions for the dislocation core field as cylindrical dilatations caused by a line defect represented by unequal force dipoles, which are in turn superposed on the Volterra field. We have instead obtained a continuum representation of the combined core and Volterra field of an isolated edge dislocation modeled in MD through a spectral method. As shown in Fig. 3, we find that a CNN, trained on a dataset generated by superposing the continuum fields of randomly-spaced GBDs, is able to accurately quantify the locations of the GBDs ***even for very high angle grain boundaries with overlapping core fields***. A sampling of the predictions for various sliding detection widows are shown for high-tilt-angle grain boundaries with $\psi = 28.06°$ and $36.86°$ in Fig. 3a and 3b. We obtain very consistent localization predictions with limited scatter for both boundaries; the average localization predictions of the CNN (green dislocation symbols) are very close to the actual dislocation location (cross symbol) at the center of the error bounding box (black). We further push the limits our CNN predictions by examining the localization capabilities when applied to a grain boundary with a very high tilt angle of $\psi = 53.13°$ in Fig. 3c. While we cannot ascertain with high confidence the ground truth location of the GBDs along this particular grain boundary, the scatter in predictions (magenta) across all sliding detection windows is still within reasonable limits, lending confidence to the average predictions (green dislocation symbols) as representative of the grain boundary dislocation structure. This machine learning approach of detecting the presence and identifying the locations of dislocations with sub-angstrom accuracies is a significant improvement over prior approaches based on Burgers circuit analyses, which are typically limited to low- and moderate-tilt-angle grain boundaries with no overlapping cores.

While we base our training/testing datasets in this work on dislocation/grain boundary structures modeled with MD simulations, we can similarly train or apply the same neural network architecture to other atomistic models of grain boundaries to predict the corresponding GBD structures, as long as a quantifiable measure of the atomistic stress tensor (stress-per-atom) near the grain boundary exists (Section 2.1). In Fig. 4a, we show that this CNN is able to detect, from the DFT stress field of a high-tilt-angle grain boundary, the presence of GBDs with true positive and true negative accuracies of 100% and 90%, respectively, along with localization accuracies of 95%, and we show the predicted GBD location on a high resolution TEM image of the same boundary in Fig. 4b.

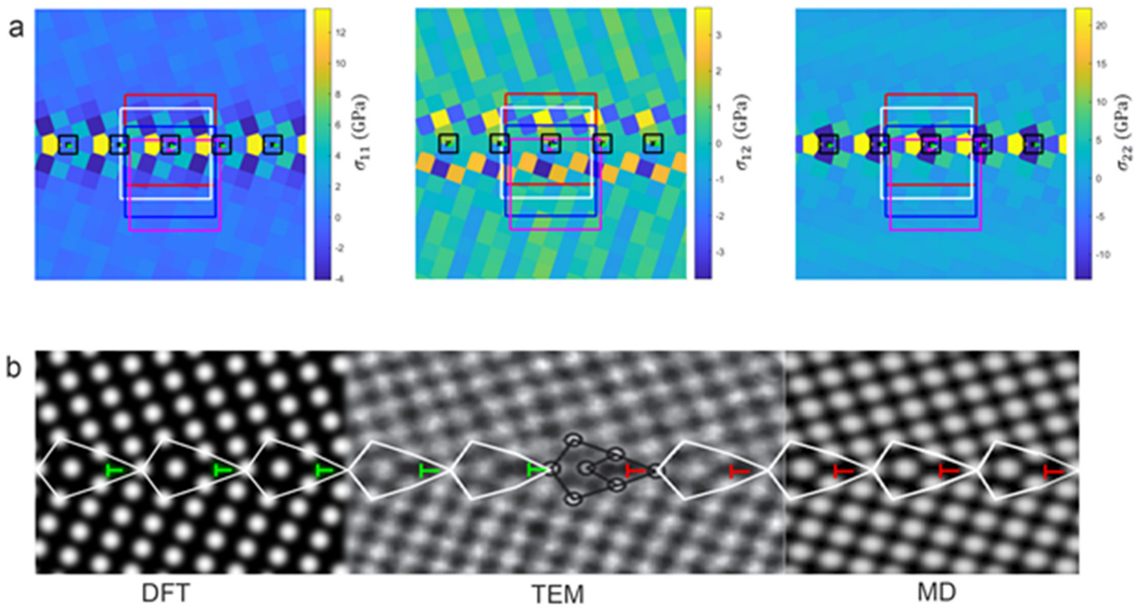

FIG. 4: DFT computations of GBDs for high-tilt-angle grain boundary with $\psi = 36.86°$. (a) Stress-per-atom computations, with colored boxes and dislocation symbols denoting sampling of detection windows for true positive edge dislocations with corresponding dislocation locations; black box: ±2 pixel error bound centered about the actual dislocation location (black cross). (b) Comparison of DFT, TEM, and MD grain boundary structures; green and red dislocation symbols: average predicted dislocation location from DFT- and MD-generated grain boundaries across all positive detection windows.